PHYSICAL REVIEW D **94,** 026011 (2016)

Crystalline geometries from fermionic vortex lattice with hyperscaling violation

Li-Ke Chen,[1,2] Hong Guo,[1] and Fu-Wen Shu[1,2,3,*]

[1]*Department of Physics, Nanchang University, Nanchang 330031, People's Republic of China*
[2]*Center for Relativistic Astrophysics and High Energy Physics, Nanchang University, Nanchang 330031, People's Republic of China*
[3]*Kavli Institute for Theoretical Physics China, Institute of Theoretical Physics, Chinese Academy of Sciences, Beijing 100190, People's Republic of China*

(Received 28 March 2016; published 28 July 2016)

We analytically consider the spontaneous formation of a fermionic crystalline geometry in a gravity background with Lifshitz scaling and/or hyperscaling violation. A fermionic vortex lattice solution sourced by the lowest Landau level has been obtained. Thermodynamic analysis shows that the fermionic vortex lattice favors an equilateral triangular configuration, regardless of the values of the Lifshitz scaling z and the hyperscaling violation exponent θ. Our results also show that the larger z or lower θ leads to deeper minima in the free energy.

DOI: 10.1103/PhysRevD.94.026011

I. INTRODUCTION

Gauge/gravity duality [1–3] has attracted a lot of attention in the past few years, especially after the discovery of consistent holographic results, RHIC experiments on the viscosity/entropy-density ratio [4–6] and more recent fruitful results of applications of holography to condensed matter physics [7–10]. Due to the nature of the duality, it is a promising way of studying gauge theories in the strongly coupled regime, where the usual perturbative methods fail to apply. Many phenomena in the condensed strongly coupled systems, such as the high-T_c superconductivity, the superfluidity and the non-Fermi liquid behavior, have been addressed in the holographic framework. However, most of these works only focus on the systems which are of conformal invariance. Triggered by Son's pioneer work on nonrelativistic holography [11], recently there has been a great interest in extending gauge/gravity duality to holographic description of QFTs without the conformal invariance. Such extension has been fulfilled to Lorentz-symmetry breaking field theories which exhibit dynamical scaling [12,13] and more recently to theories with hyperscaling violation [14,15].[1] Nevertheless, all these theories still possess translational and spatial rotational symmetries. As a consequence, many crucial features of the real world materials, say, the effect of the momentum dissipation of charge carries in optical conductivity [30,31], are still far from being achieved.

To build more realistic condensed matter system in the holographic framework, the spatial translational invariance in the bulk must be broken so as to introduce the momentum dissipation. There are several ways to achieve this:

(i) The first way is to induce a holographic lattice by imposing a spatially inhomogeneous periodic source for a scalar field coupled to an Einstein-Maxwell theory [30], or alternatively by considering the backreaction of a periodic chemical potential on the metric [31].

(ii) The second approach is achieved by introducing a uniform chemical potential into the model [32–35]. Translational invariance in these models is broken, but they have a Bianchi VII_0 symmetry, which is associated with the helical order.

(iii) The third one is to treat the massive gravity as a holographic framework of describing theories with broken translational symmetry [36–39].

(iv) The fourth mechanism was proposed in [40–42] where the translational symmetry is broken by introducing massless scalars which lead to a linear dependence on the spatial coordinates of the boundary.

(v) Recently there has been a novel approach which was first proposed in [43] and then generalized to the fermionic case [44] and gravity duals with Lifshitz and/or hyperscaling violation [45]. The bulk geometry of this model is an $\mathrm{AdS}_2 \times R^2$ space supported by a magnetic field, which breaks the translational symmetry. Systems of this type exhibit nonperturbative instabilities of a probe charged scalar field coupled to the magnetic field, and the vortex lattice can be constructed via the instabilities. Notably, a distinguished difference between the first mechanism [30,31] and this one lies in their behavior at IR. Different from the current case where the effect of the lattice could persist deep in the IR, the first case

*shufuwen@ncu.edu.cn

[1]For recent progress, please see Refs. [16–29] for an incomplete list.

cannot since the background charge carriers screen the spatially modulated chemical potential in the IR. This feature gives merit to fully understanding the formation of the vortex geometry deep in the IR. Another advantage of this approach is that the backreacted crystalline geometry can be achieved analytically.

In this paper we adopt the last approach and consider the crystalline geometry in gravity duals with Lifshitz scaling and/or hyperscaling violation, which is probed by a charged Dirac fermion. We are interested in the spontaneous formation of a fermionic crystalline geometry sourced by the lowest Landau level solutions. We analytically solve the corresponding coupled PDEs for the metric and the gauge field. We obtain the same result as [44], which is different from the one obtained in [43] where a lattice structure induced by a charged scalar condensate only corrects the background magnetic field. In the fermionic case, however, the backreaction of the fermionic lattice will lead to an emergent electric field and in turn yields an effective charge density. Furthermore, we also investigate influences of the scaling exponent and the hyperscaling violation exponent on the spontaneous formation of the crystalline geometry. To achieve this, we carefully analyze the thermodynamic quantities of the systems. Our results show that lattices with larger z or lower θ are more stable thermodynamically.

The other main motivation of this paper is to find out which configuration of the holographic vortex lattice prefers to form in our model. This is important because configuration is one of the major properties of the lattice and it provides a way to compare the holographic model with the traditional one (say, the Abrikosov lattice [46]). Most of the previous works [43–45], for the sake of simplification, made an assumption that the vortex lattice is rectangular. This is a very unnatural assumption considering the experimental result of the traditional vortex lattice which is usually triangular. In this paper, we investigate this problem very carefully. Our results show that the fermionic vortex favors an equilateral triangular configuration, regardless of the values of z and θ. This result provides an alternative confirmation of the holographic model.

The organization of this paper is as follows: in the next section we will discuss the background geometry in question. Equations of motion are obtained and the Dirac field as a probe has been considered and the corresponding Dirac equation in this background has been achieved. In Sec. III, we solve these differential equations and construct a vortex lattice solution. The radial behavior of the wave functions is also discussed. In Sec. IV we consider linear backreactions of the fermionic vortex on the background and the gauge field. Some thermodynamical variables such as free energy of the lattice will be discussed in Sec. V, where we find that the vortex lattice tends to a triangular configuration. The full fourth-order free energy strongly suggests an equilateral triangular configuration. Some thermodynamic behavior of the lattice affected by z and θ has also been discussed there. We give conclusions in the last section. Calculations of double Fourier series are given in Appendix A and the computation of the full on-shell action is given in Appendix B.

II. BACKGROUND SETUP

In this section, we will discuss the basic ingredients to build the model of a fermionic lattice with a hyperscaling violation exponent. Our starting point is the Einstein-Maxwell-dilaton (EMD) model:

$$S_1 = -\frac{1}{16\pi G}\int d^4x\sqrt{-g} \times \left[R - \frac{1}{2}(\partial\phi)^2 + V(\phi) - \frac{Z(\phi)}{4}F^2\right], \tag{1}$$

where the dilaton ϕ is dual to the scalar relevant operator of the system that drives a nontrivial renormalization group (RG) flow from the UV to the IR. It can either be a constant or running in the IR. The $U(1)$ gauge field coupled to the dilaton is required to give the anisotropic scaling. Since we are interested in spontaneous formation of the crystalline geometries, the translational invariance should be broken. In this scheme, we achieve this by placing a magnetic field along the x direction, so the gauge field is restrained as

$$F_{xy} = Q_m dx\wedge dy, \tag{2}$$

where Q_m can be viewed as the magnetic charge, and we assume that $Q_m \geq 0$ throughout this paper.

We assume that $V(\phi)$ and $Z(\phi)$ have exponential asymptotics. In particular, we are considering the following forms:

$$V(\phi) = V_0 e^{\gamma\phi}, \qquad Z(\phi) = e^{\lambda\phi}. \tag{3}$$

The model can be supported by an extremal black brane whose near-horizon geometry is given by the hyperscaling violating Lifshitz (hvLif) metric

$$ds^2 = L^2 r^\theta\left(-\frac{dt^2}{r^{2z}} + \frac{dr^2}{r^2} + \frac{dx^2+dy^2}{r^2}\right), \tag{4}$$

$$e^{\phi(r)} = e^{\phi_0} r^{-\sqrt{\theta^2-2z(\theta-2)-4}}, \tag{5}$$

$$\gamma = \frac{\theta}{\sqrt{\theta^2-2z(\theta-2)-4}}, \tag{6}$$

$$\lambda = \frac{4-\theta}{\sqrt{\theta^2-2z(\theta-2)-4}}, \tag{7}$$

$$L = \frac{Q_m e^{\lambda\phi_0}}{\sqrt{2(z-1)(2+z-\theta)}}, \tag{8}$$

$$V_0 = \frac{1}{2}(z-1)(1+z-\theta)(2+z-\theta)^2 Q_m^2 e^{(\lambda-\gamma)\phi_0}, \quad (9)$$

where z denotes the Lifshitz scaling, θ is the hyperscaling violation exponent, and $r \to 0$ and $r \to \infty$ correspond to UV and IR respectively. For simplification, we have set $\phi_0 = 0$ in the following argument.

The null energy condition imposes constraints on the allowed values for z and θ [15]:

$$\text{(i) For } 1 \le z \le 2\text{: } \theta \le 2(z-1) \quad \text{or} \quad 2 \le \theta \le 2+z, \quad (10)$$

$$\text{(ii) For } 2 \le z \le 4\text{: } \theta \le 2, \quad \text{or} \quad 2(z-1) \le \theta \le 2+z, \quad (11)$$

$$\text{(iii) For } z > 4\text{: } \theta \le 2. \quad (12)$$

In order to study the spontaneous formation of a crystalline geometry sourced by the lowest Landau levels, we consider a massive charged Dirac field as a probe in the hvLif background (4) [44]

$$S_D = \int d^4x\sqrt{-g}i\overline{\Psi}\left(\frac{1}{2}(e_a^\mu\Gamma^a\overrightarrow{D}_\mu - \overleftarrow{D}_\mu e_a^\mu\Gamma^a) - m\right)\Psi, \quad (13)$$

where $D_\mu \equiv \partial_\mu + \frac{1}{8}\omega_{ab,\mu}[\Gamma^a,\Gamma^b] + iqA_\mu$, $\overline{\Psi} = \Psi^\dagger\Gamma^t$, while $\omega_{ab,\mu}$ is the spin connection and e_a^μ is the vierbein. Before proceeding, we choose the basis for the Dirac matrices as

$$\Gamma^t = \begin{pmatrix} -i\sigma^3 & 0 \\ 0 & -i\sigma^3 \end{pmatrix}, \qquad \Gamma^r = \begin{pmatrix} 0 & -i\sigma^2 \\ i\sigma^2 & 0 \end{pmatrix},$$
$$\Gamma^x = \begin{pmatrix} \sigma^2 & 0 \\ 0 & -\sigma^2 \end{pmatrix}, \qquad \Gamma^y = \begin{pmatrix} \sigma^1 & 0 \\ 0 & \sigma^1 \end{pmatrix}, \quad (14)$$

and the chiral gamma matrix $\Gamma^5 \equiv i\Gamma^r\Gamma^t\Gamma^x\Gamma^y$.

Variation of $S_1 + S_D$ leads to the following equations of motion,

$$(\Gamma^\mu D_\mu - m)\Psi = 0, \quad (15)$$

$$\nabla_\mu(e^{\lambda\phi}F^{\mu\nu}) = j^\nu = q\langle\hat{\overline{\Psi}}\Gamma^\nu\hat{\Psi}\rangle, \quad (16)$$

$$\nabla^\mu(\partial_\mu\phi) + V_0\gamma e^{\gamma\phi} = \frac{\lambda e^{\lambda\phi}}{4}F^{\mu\nu}F_{\mu\nu}, \quad (17)$$

$$G_{\mu\nu} = T_{\mu\nu}, \quad (18)$$

where

$$T_{\mu\nu} = \frac{1}{4}g_{\mu\nu}\left(V_0 e^{\gamma\phi} - \frac{1}{2}(\partial\phi)^2\right) + \frac{1}{4}\partial_\mu\phi\partial_\nu\phi + \frac{1}{4}e^{\lambda\phi}F_{\mu\rho}F_\nu{}^\rho - \frac{1}{16}g_{\mu\nu}e^{\lambda\phi}F^2 - \frac{i}{8}[\langle\hat{\overline{\Psi}}e_{a\mu}\Gamma^a D_\nu\hat{\Psi}\rangle + \text{H.c.}] + (\mu \leftrightarrow \nu). \quad (19)$$

In deriving the above equations, we have replaced the classical fermionic currents with their quantum mechanical ones, following what Allais *et al.* did in their paper [47]. The reason is that the zero-temperature fermionic system cannot be treated as the classical gas due to Pauli's exclusion principle. Therefore, as one considers the back-reaction of the charged fermions on the holographic geometry, the current generally cannot be treated as the classical one.[2]

In order to impose the boundary conditions, it is convenient to introduce two sets of projection operators [50],

$$P_\pm = \frac{1}{2}(1 \pm \Gamma^r), \qquad Q_{(\pm)} = \frac{1}{2}(1 \pm i\Gamma^x\Gamma^y), \quad (20)$$

under which the spinor can be decomposed into four components $\Psi^\pm_{(\pm)}$. $\Psi^-_{(\pm)}$ are interpreted as sources, while $\Psi^+_{(\pm)}$ are responses. The subscript $(\pm)$ refers to spin-up and spin-down states respectively.

Following [44], the boundary conditions can be imposed as the following:

(i) At the UV, we require that $\Psi^- = 0$ or $\Psi^+ = 0$ for standard or alternative quantization respectively. After adding a boundary term to the action such that it has a well-defined variation principle, the UV boundary condition can be translated into the following form:

$$\begin{cases} \xi_+ = 0, \chi_- = 0, & \text{for standard quantization,} \\ \xi_- = 0, \chi_+ = 0, & \text{for alternative quantization.} \end{cases} \quad (21)$$

where $\xi_\pm = \Psi^+_{(+)} \pm \Psi^+_{(-)}$, $\chi_\pm = \Psi^-_{(+)} \pm \Psi^-_{(-)}$.

(ii) At the IR boundary, as the background metric does not include horizon, it is necessary to consider a cutoff in the IR boundary if we want to obtain a nontrivial solution for the fermion in the entire bulk geometry. One possible choice is to impose a hard wall that abruptly cuts the geometry at some finite $r = r_0$. After considering the variation principle, our boundary condition on the hard wall is the same as the one given in [44]:

[2]There is another way of dealing with this current. One can treat the fermions as an ideal fluid and use a fermionic equation of state as Hartnoll *et al.* did in their electron star papers [48,49].

$$\begin{cases} \tilde{\xi}_- = 0, \tilde{\chi}_+ = 0, & \text{for standard quantization,} \\ \tilde{\xi}_+ = 0, \tilde{\chi}_- = 0, & \text{for alternative quantization,} \end{cases} \tag{22}$$

where

$$\begin{pmatrix} \tilde{\xi}_+ \\ \tilde{\xi}_- \end{pmatrix} = \begin{pmatrix} \cos\frac{\vartheta}{2} & \sin\frac{\vartheta}{2} \\ \sin\frac{\vartheta}{2} & -\cos\frac{\vartheta}{2} \end{pmatrix} \begin{pmatrix} \Psi^+_{(+)} \\ \Psi^+_{(-)} \end{pmatrix},$$
$$\begin{pmatrix} \tilde{\chi}_+ \\ \tilde{\chi}_- \end{pmatrix} = \begin{pmatrix} -\cos\frac{\vartheta}{2} & \sin\frac{\vartheta}{2} \\ \sin\frac{\vartheta}{2} & \cos\frac{\vartheta}{2} \end{pmatrix} \begin{pmatrix} \Psi^-_{(+)} \\ \Psi^-_{(-)} \end{pmatrix},$$

where $\vartheta \in (-\pi, \pi]$ is a chiral angle.

III. VORTEX LATTICE SOLUTION

A. Droplet solution

In this subsection, we will discuss the fermionic vortex lattice with hyperscaling violation exponent. According to [44], the IR instability will lead to a crystalline ground state. So it is convenient to obtain a degenerated $\Psi = 0$ solution with a vortex lattice solution.

To proceed, we consider the backreaction of the fermionic field on the background which can be achieved by expanding the fermionic field and the gauge field around the critical point,

$$\Psi(\mathbf{x}, r, t) = \epsilon\Psi_1(\mathbf{x}, r, t) + \epsilon^3\Psi_3(\mathbf{x}, r, t) + \cdots \tag{23}$$

$$A_\mu(\mathbf{x}, r) = A^{(0)}_\mu(\mathbf{x}, r) + \epsilon^2 A^{(2)}_\mu(\mathbf{x}, r) + \epsilon^4 A^{(4)}_\mu(\mathbf{x}, r) + \cdots. \tag{24}$$

Neglecting the backreaction of Ψ on the gauge sector, as well as rescaling the fermionic field $\Psi_1(r, x, y) = (-h)^{-1/4}\psi(r, x, y)$, the Dirac equation in the hyperscaling violation metric is

$$(\Gamma^r\partial_r + \Gamma^x(\partial_x + iqQ_m y) + \Gamma^y\partial_y - mLr^{\frac{\theta}{2}-1})\psi = 0. \tag{25}$$

By acting $(\Gamma^\mu D_\mu + mLr^{\frac{\theta}{2}-1})$ operator on the equation, we obtain a second-order differential equation

$$\Big[\partial_r^2 + \partial_x^2 + \partial_y^2 + 2iqQ_m y\partial_x - q^2Q_m^2y^2 + iqQ_m\Gamma^y\Gamma^x - m^2L^2r^{\theta-2} - mL\left(\frac{\theta}{2} - 1\right)\Gamma^r r^{\frac{\theta}{2}-2}\Big]\psi(r, x, y) = 0. \tag{26}$$

To solve the equation, we notice that $\Gamma^y\Gamma^x$ commutes with Γ^r. As a result we can expand the field as $\psi^\pm(r, x, y) = \rho(r)g(y)e^{ikx}C_\pm$ where the simultaneous eigenstates $C_\pm$ should satisfy the condition that $i\Gamma^y\Gamma^x C_\pm = \pm C_\pm$ and $\Gamma^r C_\pm = \pm C_\pm$. Therefore the normalized $C_\pm$ can be found as

$$C_+ = \frac{\sqrt{2}}{2}\begin{pmatrix} 0 \\ 1 \\ 1 \\ 0 \end{pmatrix}, \qquad C_- = \frac{\sqrt{2}}{2}\begin{pmatrix} 1 \\ 0 \\ 0 \\ 1 \end{pmatrix}. \tag{27}$$

After doing so, Eq. (26) reduces to a set of ordinary differential equations,

$$\rho''_\pm(r) + \left(\lambda_{n_\pm} \mp mL\left(\frac{\theta}{2} - 1\right)r^{\frac{\theta}{2}-2} - m^2L^2r^{\theta-2}\right)\rho_\pm(r) = 0 \tag{28}$$

$$g''_{n_\pm}(Y) - g_{n_\pm}\left(Y^2 + \frac{\lambda_{n_\pm}}{Q_m} \pm 1\right) = 0, \tag{29}$$

where $\lambda_{n_\pm}$ are constants corresponding to Landau levels and we have introduced a new variable $Y = \sqrt{Q_m}(y + \frac{k}{Q_m})$. An interesting fact is that both Eqs. (28) and (29) are independent of the dynamical exponent z, which means that the exponent z contributes to the vortex only through a prefactor h.

The general solution of the above equation is nothing but the familiar Hermite function

$$g_{n_\pm}(Y) \sim e^{\frac{-Y^2}{2}}H_{n_\pm}(Y), \tag{30}$$

and the corresponding eigenvalues are given by $\lambda_{n_\pm} = -2Q_m(n_\pm + \frac{1}{2} \pm \frac{1}{2})$. It should be mentioned that the above Eqs. (28) and 29 are second order, while the original Dirac equation is first order. It may impose a constraint on the eigenvalues $\lambda_{n_\pm}$. It turns out in [44] that this is given by $\lambda_{n_+} = \lambda_{n_-}$, implying that $n_- = n_+ + 1 = n$. In what follows, these relations always hold. Therefore, when we refer to the Landau level it always represents n.

B. Vortex solution

It was found in [51] that the vortex lattice can be constructed from the droplet solution at the lowest Landau level. One therefore has

$$\psi_0^{\text{lat}} = \sum_{l=-\infty}^{\infty} C_l e^{ik_l x}\psi_0(y, k_l), \tag{31}$$

where $C_l \equiv e^{-i\pi\frac{a_2}{a_1}l^2}$, $k_l = \frac{2\pi l}{a_1}\sqrt{Q_m}$ and $\psi_0 = e^{-\frac{Q_m}{2}(y+\frac{k_l}{Q_m})^2}$. After using the alternative elliptic theta function

$$\Theta_3(\nu, \tau) = \sum_{l=-\infty}^{\infty} q^{l^2}Z^{2l}, \tag{32}$$

the vortex lattice solution can be rebuilt as

$$\psi_0^{\rm lat} = -e^{-\frac{Q_m y^2}{2}}\Theta_3(\upsilon,\tau), \tag{33}$$

where $q = e^{i\tau\pi}$, $Z = e^{i\pi\upsilon}$ with $\upsilon = \frac{\sqrt{Q_m}(x+iy)}{a_1}$ and $\tau = \frac{2\pi i - a_2}{a_1^2}$.

A well-known fact is that the elliptic theta function has two special properties. The first one is that Θ_3 has a pseudoperiodicity

$$\Theta_3(\upsilon+1,\tau) = \Theta_3(\upsilon,\tau), \tag{34}$$

$$\Theta_3(\upsilon+\tau,\tau) = e^{-2\pi i(\upsilon+\frac{\tau}{2})}\Theta_3(\upsilon,\tau) \tag{35}$$

implying that the function ψ_0^{lat} which depends on the form of Θ_3 has the property of the invariance of translation according to the lattice generators,

$$\vec{b}_1 = \frac{1}{\sqrt{Q_m}}a_1\partial_x, \tag{36}$$

$$\vec{b}_2 = \frac{1}{\sqrt{Q_m}}\left(\frac{2\pi}{a_1}\partial_y + \frac{a_2}{a_1}\partial_x\right). \tag{37}$$

The second property is that the Θ_3 function will vanish at

$$\vec{\chi}_{m,n} = \left(m+\frac{1}{2}\right)\vec{b}_1 + \left(n+\frac{1}{2}\right)\vec{b}_2 \quad m,n\in\mathbb{N} \tag{38}$$

and the phase of $\langle\mathcal{O}\rangle$ rotates by 2π. So the core of the vortex is located at $\vec{\chi}_{m,n}$.

C. Radial equation

Since we are focusing on the lowest Landau level solutions, we have $\lambda_+ = \lambda_- = 0$. Substituting this into Eq. (28), we get

$$\rho_\pm'' + \left[\mp mL\left(\frac{\theta}{2}-1\right)r^{\frac{\theta}{2}-2} - m^2L^2r^{\theta-2}\right]\rho_\pm(r) = 0. \tag{39}$$

Notice that equations for ρ_+ and ρ_- are related through a transformation $mL \to -mL$. Therefore one can always obtain ρ_- from ρ_+ by inverting the value of mL, and vice versa. In what follows, we only consider the equation for ρ_+, and we omit the subscript as well,

$$\rho'' - \left[mL\left(\frac{\theta}{2}-1\right)r^{\frac{\theta}{2}-2} + m^2L^2r^{\theta-2}\right]\rho(r) = 0. \tag{40}$$

1. $\theta = 0$

This case reduces to a Lifshitz spacetime without hyperscaling violation. The radial equation (40) becomes

$$\frac{\rho''(r)}{\rho(r)} + mLr^{-2} - m^2L^2r^{-2} = 0. \tag{41}$$

The above equation admits a power-law solution

$$\rho = c_1 r^{\alpha_+} + c_2 r^{\alpha_-}, \tag{42}$$

where

$$\alpha_\pm = \pm\left(mL - \frac{1}{2}\right).$$

Translating it into the fermionic field, we obtain

$$\Psi_1(r,x,y) = \frac{1}{L^{3/2}}(c_1 r^{\Delta_+} + c_2 r^{\Delta_-})\psi_0^{\rm lat}(x,y)C_+, \tag{43}$$

where $\Delta_\pm = 1 + \frac{z}{2} + \alpha_\pm$. The above solution has two radial modes. For the case where $mL > \frac{3+z}{2}$ one can only consider the standard quantization,[3] while for $mL < \frac{3+z}{2}$ the alternative quantization is also available.

2. $\theta \neq 0$

For this case, we first define a function $\varphi(r) \equiv \frac{\rho'(r)}{\rho(r)}$, and then Eq. (40) becomes a Ricatti equation,

$$\varphi'(r) + \varphi^2(r) - [(mLr^{\frac{\theta}{2}-1})' + (mLr^{\frac{\theta}{2}-1})^2] = 0, \tag{44}$$

which admits a special power-law solution,

$$\varphi_0(r) = mLr^{\frac{\theta}{2}-1}. \tag{45}$$

We therefore get an exponential form of ρ,

$$\rho(r) = \rho_0\exp\left(\frac{2mL}{\theta}r^{\frac{\theta}{2}}\right), \tag{46}$$

where $\rho_0 = \rho(r=0)$ is a constant.

Actually, making use of the special solution $\varphi_0(r)$ from Eq. (45), more general solutions of Eq. (44) can be found with the assumption $\varphi(r) = u(r) + \varphi_0(r)$. Substituting this into Eq. (44), one gets a solution for $u(r)$,

$$u(r) = \frac{\lambda\theta\exp(-(\lambda r)^{\frac{\theta}{2}})}{b\lambda\theta - 2\Gamma(\frac{2}{\theta},(\lambda r)^{\frac{\theta}{2}})}, \tag{47}$$

where b is an integration constant and

$$\lambda \equiv \left(\frac{4mL}{\theta}\right)^{\frac{2}{\theta}}. \tag{48}$$

We therefore obtain a general solution of ρ by integrating

[3]This corresponds to $\Delta_- < 0$. Since we are considering spontaneous formation of the lattice, we should turn off the source term and leave a scaling dimension of the boundary operator to be $\Delta(\Psi_1) = \Delta_+$.

$$\rho(r) = \rho_0 \exp\left(\frac{2mL}{\theta} r^{\frac{\theta}{2}} + \int u(r)dr\right). \tag{49}$$

Near the UV boundary ($r \to 0$), the above function for $\theta > 0$ can be expanded as

$$\rho(r) = d_1 + d_2 r + \mathcal{O}(r) \tag{50}$$

where

$$d_1 = \rho_0\left(1+\frac{\theta}{2}\right)\left(\frac{b\lambda\theta}{2} - \Gamma\left(\frac{2}{\theta}\right)\right), \qquad d_2 = \frac{\rho_0}{2}\left(1+\frac{\theta}{2}\right)\theta. \tag{51}$$

Translating it into the fermionic field, we obtain

$$\Psi_1(r,x,y) = \frac{1}{L^{3/2}}(d_1 r^{\Delta_-} + d_2 r^{\Delta_+})\psi_0^{\text{lat}}(x,y)C_+, \tag{52}$$

where $\Delta_\pm = \frac{6+2z-3\theta}{4} \pm \frac{1}{2}$. For the case where $3\theta - 2z > 4$ one can only consider the standard quantization, and we turn off the source term, leaving $\Delta(\Psi_1) = \Delta_+$. From now on, we pay attention to this case and for simplification we briefly denote Δ_+ as Δ.

IV. LINEAR BACKREACTIONS

In this section, the backreactions of the fermionic vortex on the metric, the gauge field and dilaton will be discussed. The backreactions are sourced by the fermions at the matter current and energy-momentum tensor at order $\mathcal{O}(\epsilon^2)$. It shows that the only nontrivial sources at order $\mathcal{O}(\epsilon^2)$ are T_{tx} and T_{ty}. So the following *Ansätze* for the backreacted metric, gauge field and dilaton, respectively, are

$$ds^2 = L^2 r^\theta\left(-\frac{dt^2}{r^{2z}} + \frac{dr^2}{r^2} + \frac{dx^2+dy^2}{r^2}\right) + L^2\epsilon^2 r^\beta[a(r,x,y)dtdx + b(r,x,y)dtdy] \tag{53}$$

$$A = Q_m y dx + \epsilon^2 r^\alpha a_2^t(r,x,y)dt \tag{54}$$

$$\phi(r,x,y) = \phi_1(r) + \epsilon^2\phi_2(r,x,y) \tag{55}$$

where $\beta = \frac{3}{2}\theta - z$, $\alpha = \frac{\theta}{2} - z + 4$ and $\phi_1(r)$ is given in (5).

At order $\mathcal{O}(\epsilon^2)$, the nontrivial Einstein equations (coming from G_{tr}, G_{tx}, G_{ty}); gauge field equation; and dilation equation are shown as (we have set $Q_m = 1$ in the following argument)

$$(\beta + 2z + 2\Delta - \theta)(\partial_x a + \partial_y b) = 0, \tag{56}$$

$$Ma = -2i[\langle\hat{\Psi}_1\partial_x\hat{\Psi}_1^\dagger\rangle - \langle\hat{\Psi}_1^\dagger\partial_x\hat{\Psi}_1\rangle - 2iy\langle\hat{\Psi}_1^\dagger\hat{\Psi}_1\rangle], \tag{57}$$

$$Mb = -2i[\langle\hat{\Psi}_0\partial_y\hat{\Psi}_1^\dagger\rangle - \langle\hat{\Psi}_1^\dagger\partial_y\hat{\Psi}_1\rangle], \tag{58}$$

$$Qa_2^t + \frac{1}{2}(\partial_x b - \partial_y a) = 2L^3\langle\hat{\Psi}_1^\dagger\hat{\Psi}_1\rangle, \tag{59}$$

$$r^2\partial_r^2\phi_2 + r(\theta - z - 1)\partial_r\phi_2 + P\phi_2 = 0, \tag{60}$$

where

$$M = \frac{\sqrt{(z-1)(2+z-\theta)}(-4-10z^2+16\Delta(\Delta+\theta)+\theta(\theta+6+6z)-z(8\Delta+6))}{\sqrt{2}}, \tag{61}$$

$$Q = -\frac{1}{4}(2z-4\Delta-\theta-8)(4\Delta+3\theta-2), \tag{62}$$

$$P = \frac{(2+z-\theta)(-32+16\theta-3\theta^2+\theta^3+z(32-16\theta+\theta^2))}{2(2z-\theta-2)(\theta-2)}. \tag{63}$$

The above equations have several nontrivial features. First of all, the equation governing ϕ_2 is completely decoupled from other variables, which means that the second-order corrections of the dilation, if it exists, are neither sourced by the vortex lattices directly nor affected through other fields like a, b and a_2^t indirectly. In other words, the vortex lattice does *not* impose any influences on the dilaton at this order. This reminds us that $\phi_2 = 0$ is a reasonable solution to (60). Secondly, all the functions except $\phi_2(r,x,y)$ are sourced by $\langle\hat{\Psi}_1^\dagger\hat{\Psi}_1\rangle$ which scales as $r^{2\Delta}$ near the boundary. It is very natural to assume that $a(r,x,y)$, $b(r,x,y)$ and $a_2^t(r,x,y)$ all scale as $r^{2\Delta}$ where Δ is given by

$$\Delta = \begin{cases} mL + \frac{1+z}{2}, & \text{for } \theta = 0, \\ 2 + \frac{z}{2} - \frac{3\theta}{4}, & \text{for } \theta > 0, \end{cases} \tag{64}$$

as what have shown in the last section. As a consequence we suppose that

$$f_i(r,x,y) = r^{2\Delta} f_i(x,y) \tag{65}$$

where $f_i(r,x,y) = a, b, a_2^t$.

Considering that the vortex lattice is periodic in both the x and y directions with periodicity $|\vec{b}_1|$ in the x direction and $|\vec{b}_2|$ in the y direction, we therefore perform the following double Fourier series:

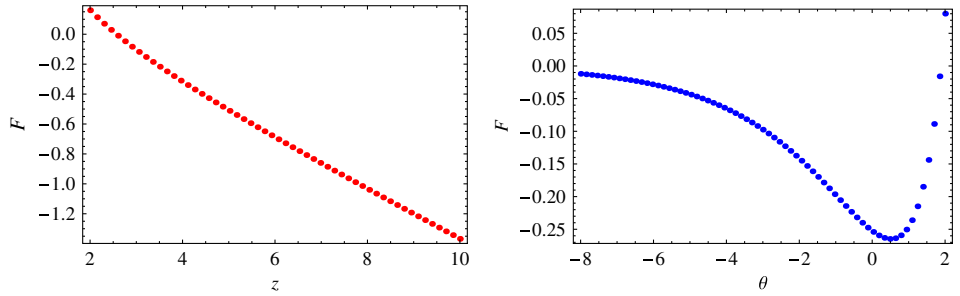

FIG. 1. The zeroth-order free energy plotted as a function of the Lifshitz scaling z (left plot) and hyperscaling violation exponent θ (right plot). It decreases (almost linearly) with increasing z as shown in the left plot and increases with increasing θ as shown in the right plot.

$$f_i(x,y)=\frac{1}{L^{3/2}}\sum_{k,l,j}a_1 e^{\frac{2\pi i k x}{|\vec{b}_1|}}e^{\frac{2\pi i j y}{|\vec{b}_2|}}e^{g(k,l,j)}\tilde{f}_i(k,l,j), \tag{66}$$

where $g(k,l,j)=-\frac{\pi^2k^2}{a_1^2}-i\pi\frac{a_2}{a_1^2}(2l-k)k-i\pi kj-\frac{a_1^2j^2}{4}$. After inserting the above series into Eqs. (56)–(60), we obtain a set of algebraic equations for $\tilde{f}_i(k,l,j)$. A trick here is that to avoid doing a double Fourier series of derivatives appearing in the equations, one should first translate them into functions of Ψ_1 or $\Psi_1^\dagger$ and their derivatives (one can find detailed calculations in the appendixes). In the end we get the following solutions:

$$\tilde{a}=\frac{ija_1}{\sqrt{\pi}M}, \tag{67}$$

$$\tilde{b}=\frac{-2i\sqrt{\pi}k}{Ma_1}, \tag{68}$$

$$\tilde{a_2^t}=W=\frac{1}{\sqrt{\pi}Q}\left(L^3+\frac{2a_1^2j^2}{M}-\frac{8\pi^2k^2}{a_1^2M}\right), \tag{69}$$

$$\phi_2=0. \tag{70}$$

Substituting the above solutions into (66) one obtains solutions in coordinate space.

V. FREE ENERGY

In order to see which configuration the vortex lattice prefers to form, in this section we would like to discuss the effects of the lattice formation on the thermodynamic functions. Particularly, we will compute corrections to the free energy of the vortex lattice solution via the on-shell value of the bulk action

$$F\sim TS_{\text{on-shell}} \tag{71}$$

where T is the energy scale. Following [43,45] we interpret r_0 as a confinement scale Λ^{-1} in the wall geometry. In this way we substitute $r_0\sim T^{-\frac{1}{z}}$ so as to get temperature dependence. Direct calculations show that

$$S^{(0)}_{\text{on-shell}}=\frac{2+5z+z^2-3\theta-3z\theta}{\theta-z-2}r^{\theta-z-2}, \tag{72}$$

$$S^{(2)}_{\text{on-shell}}=0. \tag{73}$$

Several remarkable remarks are as follows:

(i) There are vanishing corrections of free energy at the second order. This is different from the $AdS_2\times R^2$ case as shown both in fermionic crystalline geometry [44] and in scalar crystalline geometry [43], and is different even from the case where the background spacetime is a Lifshitz one with hyperscaling violation [45].

(ii) Straightforward calculations show that the free energy decreases, almost linearly, with z for fixed hyperscaling violation exponent θ, while it increases with θ for some fixed z. This indicates that the vortex lattice has more stable thermodynamic stability for larger z or lower θ. The detailed behavior can be found in Fig. 1.

A. The fourth-order free energy

Due to the vanishing free energy at the second order, we have to consider it up to fourth order. It is given by

$$S^{(4)}_{\text{on-shell}}=\frac{1}{16M^2\pi}\sum_{k,l,j=-\infty}^{\infty}e^{\frac{4\pi i k x}{|\vec{b}_1|}+\frac{4\pi i j y}{|\vec{b}_2|}+2g(k,j,l)}\times(A_1+A_2r^2)r^{8+z-\theta}, \tag{74}$$

where

$$A_1=-\frac{4L^2\pi^2k^2+L^2b_1^4j^2}{8+z-\theta}\left(56\Delta^2+4z^2+5\theta^2+14\beta^2-16\theta\beta-32\Delta\theta-10z\theta+56\Delta\beta+16z\beta+32z\Delta-8\theta+8\beta+8z+16\Delta+1+(\theta-2)\times(\theta-2z+2)-\frac{4}{L^2}-2L^2V_0\right), \tag{75}$$

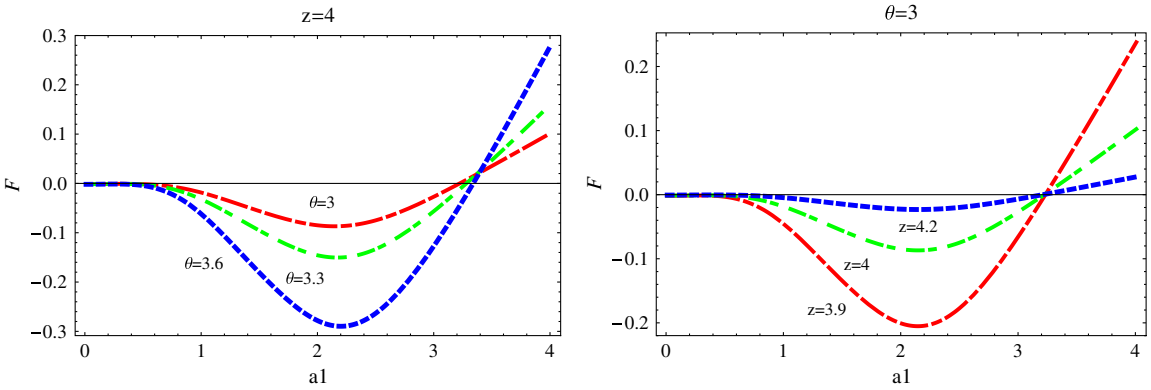

FIG. 2. The fourth-order free energy plotted as a function of a_1 with $a_2 = \frac{a_1^2}{2}$. The left plot corresponds to curves of fourth-order free energy vs a_1 for different θ, while the right one refers to the corresponding curves for different z. Both plots show a minimum located at the neighbor of $a_1 = 2$.

$$A_2 = \left\{ 56L^2\pi^2\left(\frac{4\pi^2k^4}{b_1^2} + \frac{b_1^4j^4}{b_2^2} + \frac{4\pi b_1 j^2k^2}{b_2}\right) - 32\pi M^2W^2\left[(\alpha+2\Delta)^2 - 4\pi^2\left(\frac{k^2}{b_1^2} + \frac{j^2}{b_2^2}\right)\right] - 64MW\pi^{3/2}\left(\frac{b_1^2j^2}{b_2} + \frac{2\pi k^2}{b_1}\right)\right\}\frac{1}{10+z-\theta}, \tag{76}$$

with $b_1 = |\vec{b}_1| = a_1$, $b_2 = |\vec{b}_2| = \sqrt{a_2^2 + 4\pi^2}/a_1$. As a result, up to order ϵ^4, the on-shell action is

$$S_{\text{on-shell}} \sim r_0^{\theta-z-2}[1 + \epsilon^4(A_1 r_0^{10+2z-2\theta} + A_2 r_0^{12+2z-2\theta}) + \ldots]. \tag{77}$$

The free energy is then given by

$$F \sim T^{2+\frac{2-\theta}{z}}[1 + \epsilon^4(A_1 T^{\frac{-1}{z}(10+2z-2\theta)} + A_2 T^{\frac{-1}{z}(12+2z-2\theta)}) + \ldots]. \tag{78}$$

An interesting feature at this order is that the vortex lattice favors a triangular configuration, regardless of the values of z and θ. To learn this more explicitly, a plot of free energy vs lattice constant a_1 ($a_2 = \frac{1}{2}a_1^2$) has been drawn (Fig. 2). From those figures, we see that the free energy has a minimum value for different z and θ. Remarkably, all the minima are located very close to $a_1 = 2$. It is well known that an equilateral triangular lattice has a lattice constant

$$a_1 = \frac{2\sqrt{\pi}}{3^{\frac{1}{4}}} \simeq 2.69. \tag{79}$$

There is a discrepancy between this value and our minimum location $a_1 = 2$. This discrepancy possibly comes from the fact that our on-shell action at the fourth order is not complete. The complete fourth-order on-shell action includes not only the quadratic terms of the second-order ones like a, b, a_2^t, but also those terms that are further backreacted by these backreactions a, b and a_2^t. In the present subsection we have only considered the first contributions. The second one refers to solving higher-order differential equations for fields like $\Psi_3(r,x,y)$ and $A_\mu^{(4)}(r,x,y)$ in Eqs. (23) and (24) and therefore has not yet been taken into account. Although it is complicated, it is possible to do that, following what we have done in a recent paper on vortex lattice formation of a d-wave superconductor [52]. We will confirm this point in the next subsection.

One less important observation in Fig. 2 is that it seems that a larger z or θ has a larger minimum near $a_1 = 2$. This implies that trends to form a triangular lattice decrease with increasing z and θ. For the special case $\theta = 0$, we have behavior similar to the nonvanishing ones, as plotted in Fig. 3.

B. The full fourth-order free energy

In the last subsection we find that there is a discrepancy between the lattice constant of an equilateral triangular lattice and our minimum location and argue that this discrepancy comes from the fact that our on-shell action at the fourth order

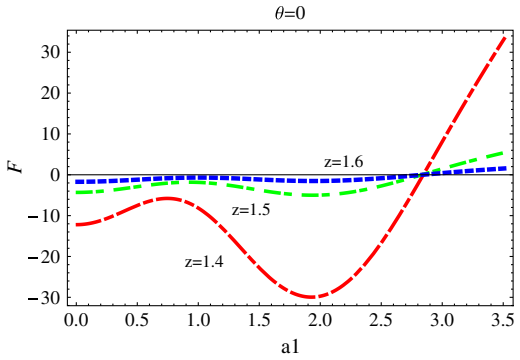

FIG. 3. The fourth-order free energy plotted as a function of a_1 with $a_2 = \frac{a_1^2}{2}$ for different z, but with fixed exponent $\theta = 0$.

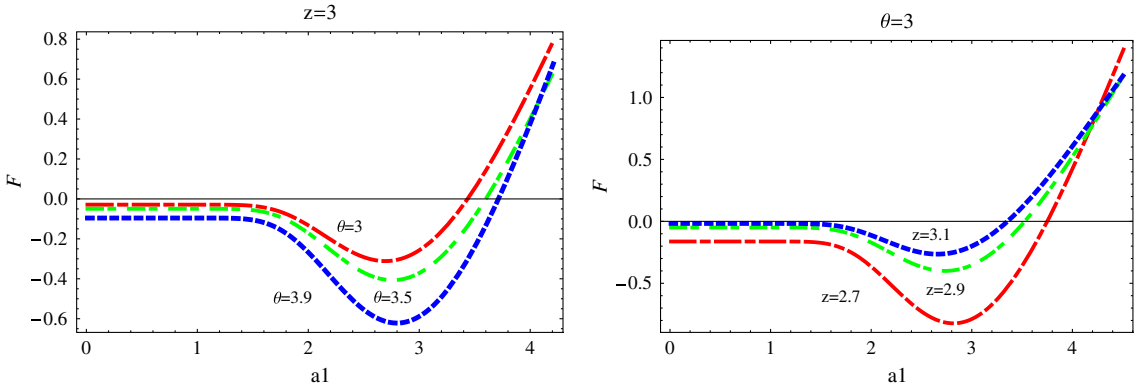

FIG. 4. The fourth-order free energy plotted as a function of a_1 with $a_2 = \frac{a_1^2}{2}$. The left plot corresponds to curves of full fourth-order free energy vs a_1 for different θ with fixed $z = 3$, while the right one refers to the corresponding curves for different z with fixed $\theta = 3$. Both plots show a minimum located in the neighborhood of $a_1 \approx 2.69$, which implies an equilateral triangular configuration.

is not complete. In this subsection we fix the discrepancy by considering the full fourth-order on-shell action, which includes the following two contributions:

(a) the quadratic terms of the second-order ones like a, b, a_2^t, which have been calculated in the last subsection;
(b) the terms that are further backreacted by these backreactions a, b and a_2^t. These terms refer to solving higher-order differential equations for fields like $\Psi_3(r,x,y)$ and $A_\mu^{(4)}(r,x,y)$ in Eqs. (23) and (24).

The main task in this subsection is to calculate the second contribution and to show that the lattice configuration is equilateral triangular.

As the first step, let us rewrite the third-order fermion field in (23) as $\Psi_3 = \Gamma^0(C_+\Psi_3^{(1)} + C_-\Psi_3^{(2)})$, where $C_\pm$ is given by (27). We find that in our following discussion we do not need the explicit expression of $\Psi_3^{(2)}$. The Dirac equation yields the equation of $\Psi_3^{(1)}$,

$$\left[\partial_r^2 + \partial_x^2 + \partial_y^2 + 2iqQ_m y\partial_x + qQ_m - q^2Q_m^2y^2 - m^2L^2r^{\theta-2} - mL\left(\frac{\theta}{2}-1\right)r^{\frac{\theta}{2}-2}\right]\Psi_3^{(1)}(r,x,y) = iq(\partial_r a_2^t)\Psi_1, \quad (80)$$

where we have assumed r is small in the rhs of the equation.

We can solve the above equation by assuming that $\Psi_3^{(1)} = \frac{r^{3\Delta-1}}{L^{3/2}}\sum_{k,m}^{\infty} e^{\frac{2\pi i(k+m)x}{b_1}} g_3(y)$. This leads to

$$g_3''(Y) - g_3(Y^2+1) = \Omega(\theta,z,k,j,l)e^{-\frac{1}{2}Y^2 + \frac{2\pi i j}{|b_2|}y} \quad (81)$$

where $Y = y + \frac{2\pi(k+m)}{b_1}$ and $\Omega(\theta,z,k,j,l) = \sqrt{2}\Delta\frac{b_1^2 i}{\pi}e^{g(k,l,j)}$. We therefore have the following approximate solution:

$$g_3(y) = (1+\Omega y)e^{\frac{1}{2}(y+\frac{2\pi(k+m)}{b_1})^2}.$$

Next one can compute the backreactions of Ψ_3 to the gauge field, the metric and the dilaton. Similar to Eqs. (53)–(55), the backreacted metric, gauge field and the dilaton at $\mathcal{O}(\epsilon^4)$ are given, respectively, by[4]

$$\begin{aligned} ds^2 = {} & L^2r^\theta\left(-\frac{dt^2}{r^{2z}} + \frac{dr^2}{r^2} + \frac{dx^2+dy^2}{r^2}\right) \\ & + L^2r^\beta[(\epsilon^2 a(r,x,y) + \epsilon^4\sigma(r,x,y))dtdx \\ & + (\epsilon^2 b(r,x,y) + \epsilon^4\chi(r,x,y))dtdy] \\ & + L^2\epsilon^4 h(r,x,y)dr^2 \end{aligned} \quad (82)$$

$$A = Q_m y dx + r^\alpha[\epsilon^2 a_2^t(r,x,y) + \epsilon^4 a_3^t(r,x,y)]dt \quad (83)$$

[4]From (17) and (18), we have

$$\begin{aligned} \left(\frac{e^{\lambda\phi}F^2}{4}\right) &= \frac{1}{\lambda}(\nabla^\mu(\partial_\mu\phi) + V_0\gamma e^{\gamma\phi})^{(4)}, R^{(4)} = -(g^{\mu\nu}G_{\mu\nu})^{(4)} \\ &= -(g^{\mu\nu}T_{\mu\nu})^{(4)} \\ &= -\left(V_0e^{\gamma\phi} - \frac{1}{4}(\partial\phi)^2 - \frac{i}{4}g^{\mu\nu}T_{\mu\nu}^{Dirac}\right)^{(4)}, \end{aligned}$$

where $T_{\mu\nu}^{\rm Dirac} = \langle\hat{\bar{\Psi}}e_{a\mu}\Gamma^a D_\nu\hat{\Psi}\rangle + \text{H.c.}$ Substituting them into (1) we get the fourth-order on-shell action from the fourth-order backreactions:

$$\begin{aligned} S_{\text{on-shell}}^{(4)} = -\int d^4x\sqrt{-g^{(0)}}\Bigg(\left(\frac{1}{\lambda}-\frac{1}{4}\right)(\partial\phi)^2 - V_0\gamma e^{\gamma\phi} \\ + \frac{i}{4}g^{\mu\nu}T_{\mu\nu}^{\rm Dirac}\Bigg)^{(4)}. \end{aligned}$$

Notice that $((\partial\phi)^2)^{(4)} = (g^{rr})^{(4)}(\partial_r\phi)^2$, and $T_{\mu\nu}^{\rm Dirac}$ only has nonzero (tx) and (ty) components, and the only nontrivial current in (16) is j^t. It therefore suggests that at order ϵ^4 we only need to consider the following backreactions: $g_{rr}^{(4)}(r,x,y), g_{tx}^{(4)}(r,x,y), g_{ty}^{(4)}(r,x,y), A_t^{(4)}(r,x,y)$ and $\phi^{(4)}(r,x,y)$.

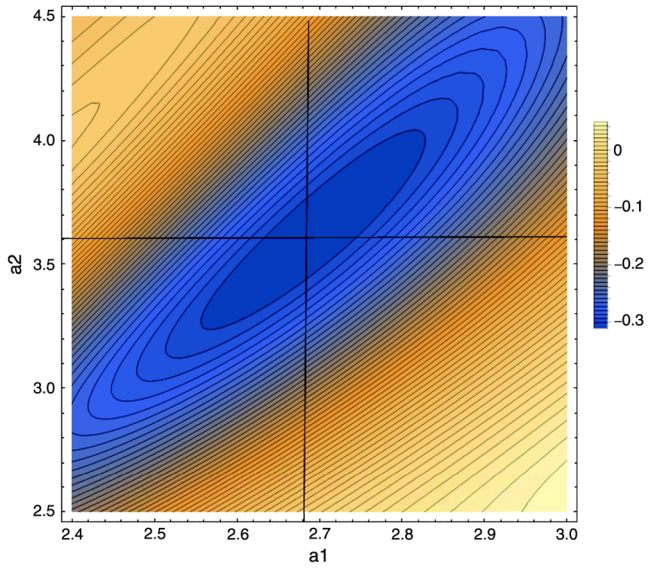

FIG. 5. The contour plot of the fourth-order free energy as a function of a_1 and a_2 for fixed $z = 3$, $\theta = 3$. The minimum is located around $a1 = 2.69$ and $a_2 = a_1^2/2 \simeq 3.61$ as expected.

$$\phi(r,x,y) = \phi_1(r) + \epsilon^2\phi_2(r,x,y) + \epsilon^4\phi_3(r,x,y). \tag{84}$$

Direct computation shows that the second contribution to the fourth-order on-shell action is given by (the details can be found in Appendix B)

$$\tilde{S}^{(4)}_{\text{on-shell}} = \frac{(4-\lambda)[\theta^2 - 2z(\theta-2) - 4]N_3}{128\lambda\pi L^2(8+z-\theta)(2N_1\theta+N_2)} r^{8+z-\theta} \times \sum_{k,j,p,q} H(k,0,j,p,q), \tag{85}$$

where $N_i (i = 1,2,3)$ and $H(k,l,j,p,q)$ are given in Appendix B.

Sum over $\tilde{S}^{(4)}_{\text{on-shell}}$ and $S^{(4)}_{\text{on-shell}}$ in (74) gives rise to the full fourth-order on-shell action. Based on this full on-shell action we can obtain the full expression of the free energy. Figure 4 is a plot of the full free energy as a function of a_1 for different parameters. The full free energy has a minimum value for different z and θ as expected. Remarkably, all the minima are located very close to $a_1 \approx 2.69$, which agrees very well with the value given in (79). The contour plot of the free energy as a function of a_1 and a_2 is also in favor of this statement as shown in Fig. 5. This strongly suggests an equilateral triangular configuration of the holographic lattice.

VI. CONCLUSIONS

In this paper we have considered the spontaneous formation of a fermionic crystalline geometry in bulk geometry with Lifshitz scaling and/or hyperscaling violation. A fermionic vortex lattice solution sourced by the lowest Landau level has been obtained. The main results of this work are as follows:

(i) The same result as [44] has been obtained, that is, different from the one in [43] where a lattice structure induced by a charged scalar condensate only corrects the background magnetic field; in our case the backreaction of the fermionic lattice will lead to an emergent electric field and an effective charge density.

(ii) Contrary to the $AdS_2 \times R^2$ case in [43] and [44], and the hyperscaling violation case in [45], the free energy in our case receives vanishing corrections at the second order.

(iii) Influences of the scaling exponent and the hyperscaling violation exponent to the spontaneous formation of the crystalline geometry are shown in Fig. 1. It can be seen that larger z or lower θ has deeper minima in the free energy.

(iv) Our calculation on the free energy shows that the fermionic vortex strongly favors an equilateral triangular configuration, regardless of the values of z and θ.

One important point is that in this work we have only considered the vortex solution sourced by the lowest Landau level where the fermionic current can be reduced to a classical one as shown in Eq. (A8). However, it is possible to generalize our results to any Landau level where the fermionic current cannot be treated classically and should be replaced by (A5) and (A6). The corresponding free energy becomes

$$F \sim T^{2+\frac{2-\theta}{z}} \sum_n [\theta(-\lambda_n) + \theta(-\lambda_n)^2\epsilon^4 \times (A_n T^{\frac{-1}{z}(10+2z-2\theta)} + B_n T^{\frac{-1}{z}(12+2z-2\theta)}) + \ldots], \tag{86}$$

where A_n and B_n are some constants.

Further investigations and generalizations of this work are possible. It is interesting to study the formation of the crystalline geometries for spacetimes with a black brane horizon. In addition, it is also possible to consider the crystalline geometry in the framework of modified gravity, such as the Hořava-Lifshitz (HL) gravity [53] proposed recently by Hořava. Indeed, it was found that HL gravity is a minimal holographic dual for the field with Lifshitz scaling [54]. Our recent works [55–57] found that various Lifshitz spacetimes are possible even without matter fields. It is of particular interest to see how to construct the crystalline geometry in this framework.

ACKNOWLEDGMENTS

This work was supported in part by the National Natural Science Foundation of China (under Grants No. 11465012 and No. 11005165), the Natural Science Foundation of Jiangxi Province (under Grant No. 20142BAB202007) and the 555 talent project of Jiangxi Province.

L.-K. Chen and H. Guo contributed equally to this paper.

APPENDIX A: DOUBLE FOURIER SERIES

In this appendix we list several key procedures in doing the double Fourier series. Firstly, we expand

$$\begin{aligned}\hat{\Psi}_1^\dagger\hat{\Psi}_1 \sim& \frac{1}{L^{3/2}}\sum_l e^{-i\pi\frac{a_2 l^2}{a_1^2}} e^{\frac{2\pi i l}{|\vec{b}_1|}x} e^{-\frac{1}{2}(y+\frac{2\pi l}{a_1})^2} \\ &\cdot \sum_{\tilde{k}=l-k} e^{i\pi\frac{a_2\tilde{k}^2}{a_1^2}} e^{-\frac{2\pi i\tilde{k}}{|\vec{b}_1|}x} e^{-\frac{1}{2}(y+\frac{2\pi\tilde{k}}{a_1})^2} \\ =& \frac{1}{L^{3/2}}\sum_{k,l} e^{-i\pi\frac{a_2}{a_1^2}[l^2-(l-k)^2]} e^{\frac{2\pi i k}{|\vec{b}_1|}x} h(y) \end{aligned} \tag{A1}$$

where $h(y)$ can be described as $\sum_j h(j)e^{\frac{2\pi i j y}{|\vec{b}_2|}}$ in which

$$\begin{aligned} h(j) =& \frac{1}{|\vec{b}_2|}\int dy h\left(\frac{y}{|\vec{b}_2|}\frac{2\pi}{a_1}\right)e^{-\frac{2\pi i j y}{|\vec{b}_2|}} \\ =& \frac{a_1}{2\sqrt{\pi}}e^{A(k,l,j)}, \end{aligned} \tag{A2}$$

where

$$A(k,l,j) = -\frac{\pi^2 k^2}{a_1^2} - i\pi kj - \frac{a_1^2 j^2}{4}.$$

We therefore have

$$\hat{\Psi}_1^\dagger\hat{\Psi}_1 \sim \frac{1}{L^{3/2}}\sum_{k,l,j}\frac{a_1}{2\sqrt{\pi}}e^{\frac{2\pi i k}{|\vec{b}_1|}x}e^{\frac{2\pi i j}{|\vec{b}_2|}y}e^{g(k,l,j)} \equiv \sum_{k,l,j}\Psi^\dagger_{k,l,j}\Psi_{k,l,j} \tag{A3}$$

where

$$\begin{aligned} g(k,l,j) =& A(k,l,j) - i\pi\frac{a_2}{a_1^2}[l^2-(l-k)^2] \\ =& -\frac{\pi^2k^2}{a_1^2} - i\pi\frac{a_2}{a_1^2}(2l-k)k - i\pi kj - \frac{a_1^2j^2}{4}. \end{aligned} \tag{A4}$$

According to [47], we have

$$\langle\hat{\Psi}_1^\dagger\hat{\Psi}_1\rangle = \Delta n_{n,k,l,j} = n_{n,k,l,j}|_{Q_m} - n_{n,k,l,j}|_{Q_m=0} = n_{n,k,l,j}, \tag{A5}$$

where

$$n_{n,k,l,j} = \sum_{n,k,l,j}\theta(-\lambda_n)\Psi^\dagger_{k,l,j}\Psi_{k,l,j}, \tag{A6}$$

and

$$\theta(x) = \begin{cases} 0, & x<0, \\ 1, & x\geq 0, \end{cases} \tag{A7}$$

is the step function and λ_n is the Landau level. For the lowest Landau level $\lambda_0 = 0$ we have

$$\langle\hat{\Psi}_1^\dagger\hat{\Psi}_1\rangle = \Delta n_{n,k,l,j} = \sum_{n,k,l,j}\Psi^\dagger_{k,l,j}\Psi_{k,l,j} = \hat{\Psi}_1^\dagger\hat{\Psi}_1. \tag{A8}$$

And we get that

$$\begin{aligned}\langle\hat{\Psi}_1\partial_y\hat{\Psi}_1^\dagger\rangle - \langle\hat{\Psi}_1^\dagger\partial_y\hat{\Psi}_1\rangle =& \frac{2\pi(-l+k+l)}{a_1}\langle\hat{\Psi}_1^\dagger\hat{\Psi}_1\rangle \\ =& \frac{2\pi k}{a_1}\langle\hat{\Psi}_1^\dagger\hat{\Psi}_1\rangle, \end{aligned} \tag{A9}$$

$$\begin{aligned}&\langle\hat{\Psi}_1\partial_x\hat{\Psi}_1^\dagger\rangle - \langle\hat{\Psi}_1^\dagger\partial_x\hat{\Psi}_1\rangle - 2iy\langle\hat{\Psi}_1^\dagger\hat{\Psi}_1\rangle \\ &= \left\{\frac{2\pi i(-2l+k)}{a_1} + \frac{4i\pi}{a_1}\left[\left(l-\frac{k}{2}\right)+\frac{ia_1^2j}{4\pi}\right]\right\}\langle\hat{\Psi}_1^\dagger\hat{\Psi}_1\rangle \\ &= -a_1 j\langle\hat{\Psi}_1^\dagger\hat{\Psi}_1\rangle, \end{aligned} \tag{A10}$$

$$\begin{aligned}\partial_x a =& \frac{2i}{M}\langle\hat{\Psi}_1\partial_x^2\hat{\Psi}_1^\dagger\rangle - \langle\hat{\Psi}_1^\dagger\partial_x^2\hat{\Psi}_1\rangle - 2iy[\langle\hat{\Psi}_1\partial_x\hat{\Psi}_1^\dagger\rangle \\ &+ \langle\hat{\Psi}_1^\dagger\partial_x\hat{\Psi}_1\rangle] = \frac{2\sqrt{\pi}k}{M}ja_1\langle\hat{\Psi}_1^\dagger\hat{\Psi}_1\rangle, \end{aligned} \tag{A11}$$

$$\begin{aligned}\partial_y b =& \frac{2i}{M}\langle\hat{\Psi}_1\partial_y^2\hat{\Psi}_1^\dagger\rangle - \langle\hat{\Psi}_1^\dagger\partial_y^2\hat{\Psi}_1\rangle \\ =& \frac{2\sqrt{\pi}k}{M}(-ja_1)\langle\hat{\Psi}_1^\dagger\hat{\Psi}_1\rangle, \end{aligned} \tag{A12}$$

$$\begin{aligned}\partial_y a =& \frac{2i}{M}\langle\partial_y\hat{\Psi}_1\partial_x\hat{\Psi}_1^\dagger\rangle + \langle\hat{\Psi}_1\partial_x\partial_y\hat{\Psi}_1^\dagger\rangle - \langle\partial_y\hat{\Psi}_1^\dagger\partial_x\hat{\Psi}_1\rangle \\ &- \langle\hat{\Psi}_1^\dagger\partial_x\partial_y\hat{\Psi}_1\rangle - 2i\langle\hat{\Psi}_1\hat{\Psi}_1^\dagger\rangle \\ &- 2iy[\langle\hat{\Psi}_1\partial_y\hat{\Psi}_1^\dagger\rangle - \langle\hat{\Psi}_1^\dagger\partial_y\hat{\Psi}_1\rangle]\rangle \\ =& -\frac{2a_1^2j^2}{M}\langle\hat{\Psi}_1^\dagger\hat{\Psi}_1\rangle, \end{aligned} \tag{A13}$$

$$\begin{aligned}\partial_x b =& \frac{2i}{M}\langle\partial_x\hat{\Psi}_1\partial_y\hat{\Psi}_1^\dagger\rangle + \langle\hat{\Psi}_1\partial_x\partial_y\hat{\Psi}_1^\dagger\rangle - \langle\partial_x\hat{\Psi}_1^\dagger\partial_y\hat{\Psi}_1\rangle \\ &- \langle\hat{\Psi}_1^\dagger\partial_x\partial_y\hat{\Psi}_1\rangle = \frac{8\pi^2k^2}{a_1^2M}\langle\hat{\Psi}_1^\dagger\hat{\Psi}_1\rangle. \end{aligned} \tag{A14}$$

APPENDIX B: FOURTH-ORDER ON-SHELL ACTION

In this appendix we would like to derive the second part of the fourth-order on-shell action. Let us substitute the *Ansatz* (82)–(84) into the equations of motion and the following differential equations are obtained (for small r):

$$(\beta+2z+4\Delta-1-\theta)(\partial_x\sigma+\partial_y\chi) = 0, \tag{B1}$$

$$M_2\sigma = -2iL^3[\langle\hat{\Psi}_1^\dagger\partial_x\hat{\Psi}_3^{(1)}\rangle - \langle\hat{\Psi}_3^{(1)}\partial_x\hat{\Psi}_1^\dagger\rangle + \langle\hat{\Psi}_3^{(1)\dagger}\partial_x\hat{\Psi}_1\rangle - \langle\hat{\Psi}_1\partial_x\hat{\Psi}_3^{(1)\dagger}\rangle], \tag{B2}$$

$$M_2\chi = -2iL^3[\langle\hat{\Psi}_1^\dagger\partial_y\hat{\Psi}_3^{(1)}\rangle - \langle\hat{\Psi}_3^{(1)}\partial_y\hat{\Psi}_1^\dagger\rangle + \langle\hat{\Psi}_3^{(1)\dagger}\partial_y\hat{\Psi}_1\rangle - \langle\hat{\Psi}_1\partial_y\hat{\Psi}_3^{(1)\dagger}\rangle], \tag{B3}$$

$$Q_2 a_3^t + \frac{1}{2}(\partial_x\chi - \partial_y\sigma) = 2L^4\langle\hat{\Psi}_1^\dagger\hat{\Psi}_3^{(1)}\rangle, \tag{B4}$$

$$r^2\partial_r^2\phi_3 + r(\theta+z-1)\partial_r\phi_3 + \left(V_0\gamma^2L^2 - \frac{\lambda\gamma}{2L^2}\right)\phi_3 = 0, \tag{B5}$$

$$rN_1\partial_r h + N_2 h = r^{2\theta}N_3(a^2+b^2), \tag{B6}$$

where

$$M_2 = 4L^2[(4\Delta-1)(4\Delta+2\beta+z-\theta-1) + (z\beta-\theta\beta+\beta^2+z\theta-\theta^2/2+4\theta-2z^2-6)] + 2L^4V_0 - \frac{L^2\theta^2}{\lambda^2} - 1, \tag{B7}$$

$$Q_2 = (4\Delta-1)(4\Delta+2\alpha+z+\theta-7) + \alpha(\alpha+z+\theta-6), \tag{B8}$$

$$N_1 = 4(\theta-2), \tag{B9}$$

$$N_2 = 8 - 2\theta^2 + 2L^2V_0 - \frac{1}{2}V_0 + \left(\frac{\theta-4}{2\lambda L}\right)^2 + \frac{Q_m^2}{2L^4}, \tag{B10}$$

$$N_3 = 2\Delta(3\theta-5\beta-2z-2-5\Delta) + \left(2z^2+3\beta\theta-\frac{5}{2}\beta^2-\frac{1}{2}\theta^2-2\beta z - 2\beta-2z-2-\frac{Q_m^2}{4L^2}\right). \tag{B11}$$

Following what we have done before, we perform a double Fourier series:

$$f_i(r,x,y) = \frac{r^{4\Delta-1}}{L^{3/2}} \times \sum_{k,l,j,m,n} e^{\frac{2\pi i(k+m-l)x}{b_1}} e^{\frac{2\pi i(j+n-k)y}{b_2}} \times e^{g_2(k,l,j,m,n)}\tilde{f}_i(k,l,j,m,n), \tag{B12}$$

where $f_i = \sigma, \chi, a_3^t$ and

$$g_2(k,j,l,m,n) = -i\pi\frac{a_2}{a_1^2}l^2 - \frac{4\pi^2}{a_1^2}(k+m-l)^2 - \frac{a_1^2}{4}(j+n-k)^2 + i\pi(k+m+l)(j+n-k). \tag{B13}$$

Meanwhile, we have the Fourier series for the source $\langle\hat{\Psi}_1^\dagger\hat{\Psi}_3^{(1)}\rangle$ for the lowest Landau level

$$\langle\hat{\Psi}_1^\dagger\hat{\Psi}_3^{(1)}\rangle = \sum_{k,l,j,m,n}\left(\frac{b_1}{2\sqrt{\pi}} - \sqrt{\pi}\Omega(\theta,z,k,j,l) \times \left[\frac{1}{2}(k+m+l) + \frac{ib_1^2}{4\pi}(j+n-k)\right]\right)\cdot \times e^{g_2(k,l,j,m,n)}e^{\frac{2\pi i(k+m-l)}{b_1}x}e^{\frac{2\pi i(j+n-k)}{b_2}y}. \tag{B14}$$

The leading contribution of the Fourier series corresponds to $l=0$ which implies from (B1) that $m=-k$, $m=n+j$. We therefore have

$$\tilde{\sigma} = \tilde{\chi} = \phi_3 = 0, \qquad \tilde{a_3^t} = \frac{Lb_1}{\sqrt{\pi}Q_2}, \tag{B15}$$

$$h(r,x,y) = \frac{r^{4\Delta+2\theta}N_3}{2N_1\theta+N_2} \times \sum_{k,j,p,q} H(k,0,j,p,q), \tag{B16}$$

where

$$H(k,l,j,p,q) \equiv \left(\frac{jqa_1^4}{\pi} + 4\pi kp\right) \times \frac{1}{L^3M^2}e^{\frac{2\pi i(k+p)}{a_1}x}e^{\frac{2\pi i(j+q)}{b_2}y} \times e^{g(k,l,j)+g(p,l,q)}. \tag{B17}$$

The second contribution to the fourth-order on-shell action is therefore given by

$$\tilde{S}^{(4)}_{\text{on-shell}} = \frac{(4-\lambda)[\theta^2-2z(\theta-2)-4]N_3}{128\lambda\pi L^2(8+z-\theta)(2N_1\theta+N_2)}r^{8+z-\theta} \times \sum_{k,j,p,q} H(k,0,j,p,q). \tag{B18}$$

[1] J. M. Maldacena, The large-N limit of superconformal field theories and supergravity, Adv. Theor. Math. Phys. **2**, 231 (1998); Int. J. Theor. Phys. **38**, 1113 (1999).

[2] S. S. Gubser, I. R. Klebanov, and A. M. Polyakov, Gauge theory correlators from non-critical string theory, Phys. Lett. B **428**, 105 (1998).

[3] E. Witten, Anti-de Sitter space and holography, Adv. Theor. Math. Phys. **2**, 253 (1998).

[4] P. Kovtun, D. T. Son, and A. O. Starinets, Holography and hydrodynamics: Diffusion on stretched horizons, J. High Energy Phys. 10 (2003) 064.

[5] A. Buchel and J. T. Liu, Universality of the Shear Viscosity in Supergravity, Phys. Rev. Lett. **93**, 090602 (2004).

[6] X.-H. Ge, Y. Matsuo, F.-W. Shu, S.-J. Sin, and T. Tsukioka, Viscosity bound, causality violation and instability with stringy correction and charge, J. High Energy Phys. 10 (2008) 009.

[7] S. A. Hartnoll, Lectures on holographic methods for condensed matter physics, Classical Quantum Gravity **26**, 224002 (2009).

[8] C. P. Herzog, Lectures on holographic superfluidity and superconductivity, J. Phys. A **42**, 343001 (2009).

[9] R.-G. Cai, L. Li, L.-F. Li, and R.-Q. Yang, Introduction to holographic superconductor models, Sci. China Phys. Mech. Astron. **58**, 060401 (2015).

[10] Y. Ling, C. Niu, J. Wu, Z. Xian, and H. Zhang, Metal-Insulator Transition by Holographic Charge Density Waves, Phys. Rev. Lett. **113**, 091602 (2014).

[11] D. T. Son, Toward an AdS/cold atoms correspondence: A geometric realization of the Schroedinger symmetry, Phys. Rev. D **78**, 046003 (2008).

[12] S. Kachru, X. Liu, and M. Mulligan, Gravity duals of Lifshitz-like fixed points, Phys. Rev. D **78**, 106005 (2008).

[13] M. Taylor, Non-relativistic holography, arXiv:0812.0530.

[14] C. Charmousis, B. Gouteraux, B. S. Kim, E. Kiritsis, and R. Meyer, Effective holographic theories for low-temperature condensed matter systems, J. High Energy Phys. 11 (2010) 151; B. Gouteraux and E. Kiritsis, Generalized holographic quantum criticality at finite density, J. High Energy Phys. 12 (2011) 036.

[15] X. Dong, S. Harrison, S. Kachru, G. Torroba, and H. Wang, Aspects of holography for theories with hyperscaling violation, J. High Energy Phys. 06 (2012) 041.

[16] Q. Pan and S.-J. Zhang, Revisiting holographic superconductors with hyperscaling violation, Eur. Phys. J. C **76**, 126 (2016).

[17] G.-Q. Li, J.-X. Mo, and X.-B. Xu, Entanglement temperature for black branes with hyperscaling violation, Mod. Phys. Lett. A **31**, 1650072 (2016).

[18] P. A. González and Y. Vásquez, Scalar perturbations of nonlinear charged Lifshitz black branes with hyperscaling violation, Astrophys. Space Sci. **361**, 224 (2016).

[19] E. Kiritsis and Y. Matsuo, Charge-hyperscaling violating Lifshitz hydrodynamics from black-holes, J. High Energy Phys. 12 (2015) 076.

[20] G. Kofinas, Hyperscaling violating black holes in scalar-torsion theories, Phys. Rev. D **92**, 084022 (2015).

[21] M. H. Dehghani, A. Sheykhi, and S. E. Sadati, Thermodynamics of nonlinear charged Lifshitz black branes with hyperscaling violation, Phys. Rev. D **91**, 124073 (2015).

[22] D. Elander, R. Lawrance, and M. Piai, Hyperscaling violation and electroweak symmetry breaking, Nucl. Phys. **B897**, 583 (2015).

[23] X.-H. Feng and W.-J. Geng, Non-Abelian (hyperscaling violating) Lifshitz black holes in general dimensions, Phys. Lett. B **747**, 395 (2015).

[24] Z.-Y. Fan and H. Lu, Electrically-charged Lifshitz space-times, and hyperscaling violations, J. High Energy Phys. 04 (2015) 139.

[25] X.-M. Kuang, E. Papantonopoulos, B. Wang, and J.-P. Wu, Dynamically generated gap from holography in the charged black brane with hyperscaling violation, J. High Energy Phys. 04 (2015) 137.

[26] A. Lucas and S. Sachdev, Conductivity of weakly disordered strange metals: From conformal to hyperscaling-violating regimes, Nucl. Phys. **B892**, 239 (2015).

[27] X.-M. Kuang, E. Papantonopoulos, B. Wang, and J.-P. Wu, Formation of Fermi surfaces and the appearance of liquid phases in holographic theories with hyperscaling violation, J. High Energy Phys. 11 (2014) 086.

[28] P. Bueno and P. F. Ramirez, Higher-curvature corrections to holographic entanglement entropy in geometries with hyperscaling violation, J. High Energy Phys. 12 (2014) 078.

[29] P. Dey and S. Roy, Interpolating solution from AdS_5 to hyperscaling violating Lifshitz space-time, Phys. Rev. D **91**, 026005 (2015).

[30] G. T. Horowitz, J. E. Santos, and D. Tong, Optical conductivity with holographic lattices, J. High Energy Phys. 07 (2012) 168.

[31] G. T. Horowitz, J. E. Santos, and D. Tong, Further evidence for lattice-induced scaling, J. High Energy Phys. 11 (2012) 102.

[32] A. Donos and J. P. Gauntlett, Holographic helical superconductors, J. High Energy Phys. 12 (2011) 091.

[33] A. Donos and J. P. Gauntlett, Black holes dual to helical current phases, Phys. Rev. D **86**, 064010 (2012).

[34] A. Donos, Striped phases from holography, J. High Energy Phys. 05 (2013) 059.

[35] A. Donos and S. A. Hartnoll, Interaction-driven localization in holography, Nat. Phys. **9**, 649 (2013).

[36] D. Vegh, Holography without translational symmetry, arXiv:1301.0537.

[37] R. A. Davison, Momentum relaxation in holographic massive gravity, Phys. Rev. D **88**, 086003 (2013).

[38] M. Blake, D. Tong, and D. Vegh, Holographic Lattices Give the Graviton an Effective Mass, Phys. Rev. Lett. **112**, 071602 (2014).

[39] M. Blake and D. Tong, Universal resistivity from holographic massive gravity, Phys. Rev. D **88**, 106004 (2013).

[40] A. Donos and J. P. Gauntlett, Holographic Q-lattices, J. High Energy Phys. 04 (2014) 040.

[41] T. Andrade and B. Withers, A simple holographic model of momentum relaxation, J. High Energy Phys. 05 (2014) 101.

[42] E. Kiritsis and J. Ren, On holographic insulators and supersolids, J. High Energy Phys. 09 (2015) 168.

[43] N. Bao, S. Harrison, S. Kachru, and S. Sachdev, Vortex lattices and crystalline geometrices, Phys. Rev. D **88**, 026002 (2013).

[44] M. R. M. Mozaffar and A. Mollabashi, Crystalline geometries from fermionic vortex lattice, Phys. Rev. D **89**, 046007 (2014).
[45] N. Bao and S. Harrison, Crystalline scaling geometries from vortex lattices, Phys. Rev. D **88**, 046009 (2013).
[46] A. A. Abrikosov, *Fundamentals of the Theory of Metals* (North-Holland, New York, 1988).
[47] A. Allais, J. McGreevy, and S. J. Suh, A Quantum Electron Star, Phys. Rev. Lett. **108**, 231602 (2012).
[48] S. A. Hartnoll and A. Tavanfar, Electron stars for holographic metallic criticality, Phys. Rev. D **83**, 046003 (2011).
[49] S. A. Hartnoll, D. M. Hofman, and A. Tavanfar, Holographically smeared Fermi surface: Quantum oscillations and Luttinger count in electron star, Europhys. Lett. **95**, 31002 (2011).
[50] S. Bolognesi, J. N. Laia, D. Tong, and K. Wong, A gapless hard wall: Magnetic catalysis in bulk and boundary, J. High Energy Phys. 07 (2012) 162.
[51] K. Maeda, M. Natsuume, and T. Okamura, Vortex lattice for a holographic superconductor, Phys. Rev. D **81**, 026002 (2010).
[52] H. Guo, F. W. Shu, J. H. Chen, H. Li, and Z. Yu, A holographic model of d-wave superconductor vortices with Lifshitz scaling, Int. J. Mod. Phys. D **25**, 1650021 (2016).
[53] P. Hořava, Quantum gravity at a Lifshitz point, Phys. Rev. D **79**, 084008 (2009).
[54] T. Griffin, P. Hořava, and C. M. Melby-Thompson, Lifshitz Gravity for Lifshitz Holography, Phys. Rev. Lett. **110**, 081602 (2013).
[55] F.-W. Shu, K. Lin, A. Wang, and Q. Wu, Lifshitz spacetimes, solitons, and generalized BTZ black holes in quantum gravity at a Lifshitz point, J. High Energy Phys. 04 (2014) 056.
[56] K. Lin, F.-W. Shu, A. Wang, and Q. Wu, High-dimensional Lifshitz-type spacetimes, universal horizons and black holes in Hořava-Lifshitz gravity, Phys. Rev. D **91**, 044003 (2015).
[57] C.-J. Luo, X.-M. Kuang, and F.-W. Shu, Lifshitz holographic superconductor in Hořava-Lifshitz gravity, Phys. Lett. B **759**, 184 (2016).